jaa Just accepted article

EuroIntervention

Title: Optical Flow Ratio for Assessing Stenting Result and Physiological Significance of Residual Disease.

Authors: Daixin Ding, MSc; Wei Yu, BSc; Hélène Tauzin, PhD; Giovanni Luigi De Maria, M.D, PhD; Peng Wu, BSc; Fan Yang, BSc; Rafail A. Kotronias, MBChB, MSc; Dimitrios Terentes-Printzios, M.D, PhD; Mathias Wolfrum, M.D; Adrian P. Banning, MBBS, M.D; Nicolas Meneveau, M.D, PhD; William Wijns, M.D, PhD; Shengxian Tu, PhD

DOI: 10.4244/EIJ-D-21-00185

Citation: Ding D, Yu W, Tauzin H, De Maria GL, Wu P, Yang F, Kotronias RA, Terentes-Printzios D, Wolfrum M, Banning AP, Meneveau N, Wijns W, Tu S. Optical Flow Ratio for Assessing Stenting Result and Physiological Significance of Residual Disease. *EuroIntervention* 2021; Jaa-910 2021, doi: 10.4244/EIJ-D-21-00185

Manuscript submission date: 23 February 2021

Revisions received: 16 May 2021

Accepted date: 03 June 2021

Online publication date: 08 June 2021

Optical Flow Ratio for Assessing Stenting Result and Physiological Significance of Residual Disease

Daixin Ding[1,2*], MSc; Wei Yu[1*], BSc; Hélène Tauzin[3], PhD; Giovanni Luigi De Maria[4], MD, PhD; Peng Wu[1], BSc; Fan Yang[1], BSc; Rafail A. Kotronias[4], MBChB, MSc; Dimitrios Terentes-Printzios[4], MD, PhD; Mathias Wolfrum[4], MD; Adrian P. Banning[4], MBBS, MD; Nicolas Meneveau[3], MD, PhD; William Wijns[2], MD, PhD; Shengxian Tu[1,5], PhD

1. Biomedical Instrument Institute, School of Biomedical Engineering, Shanghai Jiao Tong University, Shanghai, China

2. The Lambe Institute for Translational Medicine and Curam, National University of Ireland Galway, Ireland

3. Department of Cardiology, University Hospital Jean Minjoz, Besançon, France

4. Oxford Heart Centre, John Radcliffe Hospital, Oxford University Hospitals, NHS Foundation Trust, Oxford, United Kingdom

5. Department of Cardiology, Fujian Medical University Union Hospital, Fuzhou, China

*The first two authors equally contributed

Short Title: OFR in predicting post-PCI FFR

Address for Correspondence

Shengxian Tu, PhD, FACC, FESC

Room 123, Med-X Research Institute

Shanghai Jiao Tong University

No. 1954, Hua Shan Road, Xuhui District

Shanghai 200030, China

E-mail: sxtu@sjtu.edu.cn

Abstract

Background: Optical flow ratio (OFR) is a novel method for fast computation of fractional flow reserve (FFR) from optical coherence tomography (OCT) images.

Aims: We aimed to evaluate the accuracy of OFR in predicting post-percutaneous coronary intervention (PCI) FFR and to evaluate the impact of stent expansion on within-stent OFR pressure drop (In-stent OFR).

Methods: Post-PCI OFR was computed in patients with both OCT and FFR interrogation immediately after PCI. Calculation of post-PCI OFR (called simulated residual OFR) from pre-PCI OCT pullbacks after elimination of the stenotic segment by virtual stenting was performed in a subgroup of patients who had pre-PCI OCT images. Stent underexpansion was quantified by the minimum expansion index (MEI) of the stented segment.

Results: A total of 125 paired comparisons between post-PCI OFR and FFR were obtained in 119 patients, among which simulated residual OFR was obtained in 64 vessels. Mean post-PCI FFR was 0.92 ± 0.05. Post-PCI OFR showed good correlation ($r = 0.74$, $p<0.001$) and agreement (mean difference = -0.01 ± 0.03, $p = 0.051$) with FFR. The accuracy in predicting post-PCI FFR≤0.90 was 84% for post-PCI OFR. Simulated residual OFR significantly correlated with post-PCI FFR ($r = 0.42$, $p<0.001$). MEI showed moderate correlation ($r=-0.49$, $p<0.001$) with In-stent OFR.

Conclusions: Post-PCI OFR showed good diagnostic concordance with post-PCI FFR. Simulated residual OFR significantly correlated with post-PCI FFR. Stent underexpansion significantly correlated with in-stent pressure drop.

Keywords: ACS / NSTE-ACS; Fractional flow reserve; Optical coherence tomography; Stable angina

Condensed Abstract

We evaluated the accuracy of OCT-based OFR in predicting post-PCI FFR and the impact of stent expansion on in-stent pressure drop. Post-PCI OFR was computed in patients with both post-PCI OCT and FFR measurements. Simulated residual OFR from pre-PCI OCT images after eliminating stenotic segment by virtual stenting was computed. The accuracy in predicting post-PCI FFR≤0.90 was 84% for post-PCI OFR. Simulated residual OFR significantly correlated with FFR ($r=0.42$, $p<0.001$). Minimum expansion index significantly correlated with in-stent pressure drop ($r=-0.49$, $p<0.001$). In conclusion, post-PCI OFR had good diagnostic concordance with post-PCI FFR. Stent underexpansion was associated with in-stent pressure drop.

Abbreviations and Acronyms

AUC = area under the curve

DS% = percent diameter stenosis

FFR = fractional flow reserve

ICCa = intraclass correlation coefficient for the absolute value

MEI = minimum expansion index

MLA = minimal lumen area

NHPR = non-hyperemic pressure ratio

NSTE-ACS = non-ST-segment elevation acute coronary syndromes

OCT = optical coherence tomography

OFR = optical flow ratio

PCI = percutaneous coronary intervention

QCA = quantitative coronary angiography

ROC = receiver-operating characteristic

Introduction

Intracoronary optical coherence tomography (OCT) imaging allows detailed assessment of coronary lumen, plaque morphology, stent apposition and expansion during percutaneous coronary intervention (PCI) [(1)]. Fractional flow reserve (FFR) can be used to assess the functional result immediately after PCI [(2)], with reported implications in terms of long-term outcomes [(3)]. Studies have advocated the use of both FFR and OCT to optimize coronary interventions and to validate the final interventional result [(4)]. However, this approach requires two disposables and separate invasive diagnostic tests (namely OCT and FFR), with increased procedural complexity, time and cost and for this reason, it is not a viable option for most health care systems.

Recently, optical flow ratio (OFR), an OCT-based method for fast computation of FFR, not requiring induced hyperemia or use of pressure wire, has been validated in *de novo* lesions or in-stent restenosis with high diagnostic concordance with FFR [(5-7)]. However, the role of post-PCI OFR in evaluating coronary physiology immediately after PCI has not been fully investigated. We have developed calculation of post-PCI OFR (called simulated residual OFR) from pre-PCI OCT run after elimination of the stenotic segment by virtual stenting. Whether simulated residual OFR can be used to predict what will be the physiological result after treating the target lesion needs to be established as well.

The aims of the present study were to validate: 1) the accuracy of post-PCI OFR computation compared to wire-based post-PCI FFR measurement; 2) the relationship between simulated residual OFR and post-PCI FFR; and 3) the impact of stent expansion and apposition on

in-stent pressure drop derived from OFR pullback.

Methods

Study design and patient population

The present study is a post-hoc analysis of combined datasets from the DOCTORS (Does Optical Coherence Tomography Optimize Results of Stenting, NCT01743274) study and the OxOPT-PCI (The Oxford Optimisation of PCI Study, NCT03111940) study. The multicenter DOCTORS study was a prospective clinical trial randomizing patients with non-ST-segment elevation acute coronary syndromes (NSTE-ACS) to either OCT-guided or angiography-guided PCI, with final post-PCI FFR as the primary endpoint [8]. The OxOPT-PCI study was a prospective, single-center, observational trial aimed to investigate the impact of a combined FFR and OCT measurements strategy on PCI optimization for patients undergoing complex PCI [9]. Detailed study design, endpoints and inclusion and exclusion criteria have been published elsewhere [8, 9].

All imaging data including coronary angiography and OCT images were sent to an independent academic core laboratory (CardHemo, Med-X Research Institute, Shanghai Jiao Tong University, China) for analysis. Post-PCI OFR analyses were performed in all selected post-PCI OCT images, except when severe artifacts or poor image quality precluded clear visualization of the coronary lumen. However, post-PCI OFR analyses were excluded from comparison with post-PCI FFR if any of the following was present: 1) vessel spasm or injury were present during post-PCI OCT imaging or FFR measurement; 2) myocardial bridge was present in the interrogated vessel or substantial thrombosis was identified by post-PCI OCT; 3) post-PCI OCT pullback did not cover the entire stented segment or in the presence of any

residual lesion(s) outside the stented segment. Specifically, if there was residual stenosis between the optical sensor and the pressure sensor, post-PCI OFR of the interrogated vessel had to be excluded from comparison with post-PCI FFR. For vessels with suboptimal post-PCI FFR (≤0.90) and/or OCT results that underwent further PCI optimization in the OxOPT-PCI study [9], paired post-PCI FFR and OFR comparisons were performed both before and after PCI optimization. For vessels without further optimization, the OCT pullback image acquired at completion of the procedure, when no further additional interventions were performed, was used for post-PCI OFR computation to be compared with final FFR value. For each interrogated vessel, simulated residual OFR was assessed using pre-PCI OCT image pullbacks, when available.

The study complied with the Declaration of Helsinki for investigation in human beings and the study protocol was approved by the institutional review board. All patients provided informed consent for enrolment in the institutional database for potential future analyses.

OCT acquisition

Details of OCT images acquisition and analysis [8-12] are described in **Supplementary Material**.

Computation of post-PCI OFR

OFR analyses were performed using the OctPlus software (version 2.0, Pulse Medical

Imaging Technology, Shanghai, China) by two experienced analysts who were blinded to FFR and clinical data. Previous studies reported low intra- and inter-observer variability in OFR analysis [7]. Detailed methodologies for OFR computation have been published elsewhere [5]. In summary, lumen contours were delineated and reconstructed in 3D. The side branches ostia were reconstructed and the reference lumen size incorporating the step-down phenomenon across bifurcations was quantified [5]. Stent struts were automatically detected using a deep learning-based algorithm [13] and combined with the lumen geometry to compute OFR pullback along the interrogated vessel. The OFR value at the distal location of the interrogated vessel was used for comparison with FFR. The pressure drop along the stented segments (denoted as In-stent OFR) was calculated as drop of OFR value within the stent (**Central Illustration**). For sequential stenoses requiring two OCT pullbacks, both were combined for OFR computation using the previously described methodology [7].

Computation of simulated residual OFR by virtual stenting

Central Illustration shows the computation of simulated residual OFR from pre-PCI OCT images by virtual stenting. Firstly, the pre-PCI OFR value of the interrogated vessel was calculated. Subsequently, the proximal and distal landmarks of the intention-to-treat lesion were selected according to the proximal and distal edges of the implanted stent(s) from post-PCI OCT pullback image. Assuming that the identified lesion was completely resolved by virtual stenting and no residual pressure drop was left behind, an OFR value without the impact of the virtually-treated lesion, namely simulated residual OFR, was reported by the

software. The simulated residual OFR, obtainable prior to PCI, was developed to provide an estimate of the maximally achievable post-PCI FFR.

Quantification of stent apposition and expansion

Stent apposition and expansion were quantified based on 3D reconstruction of the stent struts [13] and lumen geometry (**Central Illustration**). Significant stent malapposition was quantified as the total number of struts with strut-to-lumen distance above 200 μm [14]. Stent expansion index was calculated in each cross-section along the stented segment as: (stent area / reference lumen area) × 100% (**Central Illustration**). The method for deriving reference lumen was detailed by Yu et al. [5]. Briefly, the cut-plane perpendicular to the side branch centerline was reconstructed and the area of the side branch ostium was computed. Bifurcation fractal laws were then applied to calculate the reference vessel size with the step-down phenomenon when crossing bifurcations. The minimum expansion index (MEI) along the entire stented segment was used to quantify stent underexpansion. The differences in quantifying stent expansion between our method and a previous method [15] are shown in **Supplementary Figure 1**.

FFR measurement and analysis

Details for FFR measurement were reported in the main studies [8, 9, 16]. Fractional flow reserve was measured using a coronary pressure guidewire (St. Jude Medical, Saint Paul, MN,

USA). Pressure equalization was performed at the guiding catheter tip before advancing the pressure wire beyond the stenosis. After administration of intracoronary nitrates, maximal hyperemia for FFR measurement was induced using intravenous adenosine at 140 mg kg^{-1} min^{-1}, or intracoronary bolus of adenosine of 150 μg, followed by a flush of 10 ml of isotonic saline. The ratio between distal coronary pressure (Pd) and aortic pressure (Pa) during maximal hyperemia was calculated as the FFR value. The pressure sensor was pulled back at the tip of the guiding catheter to exclude pressure drift.

FFR tracings were analyzed at the participating centers in the DOCTORS and OxOPT-PCI studies [8, 9]. After blinded completion of all OFR analyses and subsequent screening for comparison with post-PCI FFR, FFR values were disclosed to the core laboratory.

Quantitative Coronary Angiography

All angiograms were analyzed using AngioPlus Core (Pulse Medical Imaging Technology, Shanghai, China) in the core laboratory. For each interrogated vessel, the post-PCI angiographic view with minimal vessel overlap at the interrogated segment and its side branches was selected for analysis.

Statistical analysis

Continuous variables were tested for normal distribution by Kolmogorov-Smirnov test and were reported as mean ± standard deviation if normally distributed or as median [quartiles] if

non-normally distributed. Categorical variables were reported as counts (percentage). Spearman's correlation coefficient was used for correlation analysis. Linear regression analysis was used to determine the proportional bias and constant bias between paired variables. Bland-Altman analysis was used to test the agreement between different continuous variables. Comparison of the limit of agreement between vessels with intraveneous or intracoronary adenosine infusion was performed by F-test. The between-center heterogeneity for assessment of the mean agreement between post-PCI OFR and FFR was tested by I^2 statistics.

The area under the curve (AUC) by receiver-operating characteristic (ROC) curve analysis by Delong method was used to compare the accuracy of post-PCI OFR and minimal lumen area (MLA) in predicting post-PCI FFR≤0.90 [3]. The Youden index was used as the criterion to determine the best cut-off value for MLA in predicting post-PCI FFR≤0.90. All statistical analyses were performed with MedCalc (version 14.12, MedCalc Software, Ostend, Belgium). A 2-sided value of $p<0.05$ was considered as statistically significant.

Results

Baseline clinical and lesion characteristics

A total of 120 patients from the OCT-guided PCI group within the DOCTORS study and 35 patients in the OxOPT-PCI study were screened. In the core laboratory, 12 OCT pullbacks were excluded due to imaging artifacts (n=11) or suboptimal OCT blood clearance (n=1). Thirty pullbacks were excluded from comparison with FFR according to the exclusion criteria, resulting in 119 vessels in 119 patients with 125 pullbacks for paired comparison of post-PCI OFR and FFR. Among 93 patients who also had pre-PCI OCT images, 29 pullbacks were excluded from simulated residual OFR analysis, resulting in 64 vessels with paired simulated residual OFR, post-PCI OFR and FFR comparison (**Figure 1**). Baseline demographic and vessel characteristics are demonstrated in **Table 1** and **Supplementary Table 1**. OCT-detected qualitative and quantitative features are shown in **Supplementary Table 2**.

Accuracy of post-PCI OFR in predicting post-PCI FFR

FFR had a mean of 0.92±0.05, OFR had a mean of 0.93±0.05. FFR≤0.90 and OFR≤0.90 was identified in 36 (28.8%) and 28 (22.4%) pullbacks, respectively. **Supplementary Figure 2** shows the cumulative frequency of post-PCI OFR and FFR.

Post-PCI OFR showed good correlation (r=0.74, p<0.001) and excellent agreement (mean difference=-0.01±0.03, p=0.051, range from -0.10 to 0.10) with FFR (**Figure 2**). The

agreement between post-PCI OFR and FFR was similar in vessels with intravenous or intracoronary adenosine infusion (standard deviation of the difference=0.03 versus 0.04, p=0.132). The I^2 statistic for assessment of the mean agreement between post-PCI OFR and FFR was 0.00 (p=0.765), indicating that the between-center variance component was small enough to be ignored.

Using a cut-off value of ≤0.90 [3] for identifying suboptimal stenting result by physiological standard, the accuracy of post-PCI OFR in predicting post-PCI FFR was 84% (95% CI: 77 to 91%), with 22 true positives, 83 true negatives, 6 false positives, and 14 false negatives. The sensitivity, specificity, positive predictive value, negative predictive value, positive likelihood ratio, and negative likelihood ratio for post-PCI OFR≤0.90 to identify post-PCI FFR≤0.90 was 61%, 93%, 79%, 86%, 9.1, and 0.42, respectively (**Table 2**). The diagnostic accuracy of post-PCI OFR ≤0.90 in predicting post-PCI FFR ≤0.90 was independent of the presence of OCT-detected stent malapposition, stent underexpansion, tissue protrusion, thrombi, stent edge dissection, and incomplete lesion coverage (**Supplementary Figure 3**). The AUC for predicting suboptimal stenting result was significantly higher for post-PCI OFR than OCT-derived MLA in the entire interrogated vessel (0.89 versus 0.74, difference=0.15 [95% CI: 0.07 to 0.23], p<0.001) (**Figure 3**). The best cut-off value for MLA in determining post-PCI FFR≤0.90 defined by Youden index was 3.28 mm^2.

Influence of stent expansion and apposition on in-stent pressure drop

In-stent OFR had a median of 0.03 [0.02 to 0.05]. Compared to vessels with low In-stent

OFR (≤0.03), vessels with high In-stent OFR (>0.03) had significantly lower MEI (57% versus 67%, p<0.001) and higher stent malapposition (9 versus 2, p=0.003). There was significant correlation between MEI and In-stent OFR (r=-0.49, p<0.001), and weak but significant correlation between stent malapposition and In-stent OFR (r=0.27, p=0.002) (**Supplementary Figure 4**).

Accuracy of simulated residual OFR in predicting post-PCI FFR

In 64 vessels with paired simulated residual OFR, post-PCI OFR and FFR analysis, pre-PCI OFR had a mean value of 0.74±0.08 and simulated residual OFR was 0.97±0.03. Simulated residual OFR showed moderate but significant correlation (r=0.42, p<0.001) and satisfactory agreement (mean difference=0.04±0.04, p<0.001) with post-PCI FFR (**Figure 4**). The correlation between simulated residual OFR and post-PCI FFR was significantly better in vessels with residual stenosis of ≥30% DS% by QCA (r=0.78, p=0.003) than in the absence of residual stenosis (r=0.28, p=0.048, difference=0.50, p=0.038). The accuracy of simulated residual OFR≤0.90 for predicting post-PCI FFR≤0.90 was 80% (95% CI: 70 to 90%), with 2 true positives, 49 true negatives, 1 false positive, and 12 false negatives (**Supplementary Table 3**).

Discussion

The main findings of the study are summarized as follows: 1) post-PCI OFR shows good correlation and excellent agreement with post-PCI FFR; 2) the diagnostic ability of post-PCI OFR in predicting post-PCI FFR is significantly better than OCT-derived MLA; 3) simulated residual OFR shows significant correlation with post-PCI FFR and the correlation is higher in vessels with residual stenosis of ≥30% DS% by QCA; 4) the accuracy in predicting post-PCI FFR≤0.90 is 84% for post-PCI OFR; 5) stent underexpansion quantified by MEI significantly correlated with in-stent pressure drop derived from OFR pullback.

The present analysis represents the first attempt to investigate the accuracy of post-PCI OFR in predicting wire-based post-PCI FFR by combining data from two independent datasets. The good agreement between post-PCI OFR and FFR might be explained by two factors. First, the reference lumen size incorporating the step-down phenomenon across bifurcations was reconstructed. This contributed to more accurate reconstruction of the healthy coronary lumen and the estimated downstream flow [5]. Second, stent struts were automatically delineated and reconstructed in 3D, contributing to a detailed and accurate geometrical model. The good correlation between post-PCI OFR and FFR was also observed in a recent single-center study with 103 intermediate coronary lesions undergoing successful PCI [17]. Of note, in post-PCI datasets, OFR and FFR values show a narrow range and skewed distribution towards normal values (see **Supplementary Figure 2**). Although there is no consensus yet as to the ideal post-PCI functional cut-off value [18], the ability of post-PCI OFR to predict post-PCI FFR ≤0.90 is clinically useful with an AUC of 0.84.

Before the advent of OFR, a coronary angiography-based computational FFR method, quantitative flow ratio (QFR), has been developed and validated with good diagnostic performance with FFR [19]. The comparison between OFR and QFR in de novo lesions and in-stent restenosis has been previously reported [6, 7]. In post-PCI settings, OFR can be superior in assessing stenting results, especially in case of complex lesion types, since OCT has the advantage of a clear visualization of essential morphological features such as stent expansion and apposition compared to angiography. The average analysis time for post-PCI OFR on each OCT pullback was reported to be 68±14 seconds [17]. Obtained in short analysis time, post-PCI OFR analysis enables simultaneous evaluation of stent deployment and its physiological impact immediately after OCT imaging without additional instrumentation. Stent underexpansion and malapposition can also be correlated with virtual pressure pullback along the stented segment, providing a strong rationale for PCI optimization.

As a novel finding, the present study reports a significant correlation between simulated residual OFR and post-PCI FFR, indicating the potential for simulated residual OFR to predict functional PCI result by anticipating the degree of residual ischemia after an "optimally successful" treatment of the index stenosis. In clinical practice, the ability to predict the physiological impact of PCI prior to proceeding with implantation of the selected stent length and size has several potential implications. As intracoronary imaging with OCT allows detailed morphological measurements including lesion length, reference vessel dimensions and plaque composition including calcification, simulated residual OFR could be of interest to select the best stenting landmark and reference dimensions to obtain the optimal

functional result, providing an ideal post-PCI OFR target to be reached by stent implantation and optimization. A suboptimal simulated residual OFR would indicate that the total ischemic burden is unlikely to be optimally reduced by PCI itself, and could identify patients who may not benefit from percutaneous revascularization. The efficacy of simulated residual OFR shall be further investigated in future prospective studies enrolling patients with more complex lesions including diffuse or serial lesions.

A significant difference between post-PCI OFR and simulated residual OFR can be explained by not just residual disease outside the stented segment, but also by stent-related mechanical issues (e.g. stent underexpansion and malapposition). While simulated residual OFR assumes no pressure drop across the stented segment by virtual stenting, a residual in-stent pressure drop (median of 0.03) was present in a number of post-PCI OFR pullbacks. Therefore, simulated residual OFR will be most useful in vessels with serial lesions or diffuse disease. For target vessels without residual stenosis, simulated residual OFR will not be able to predict the post-PCI FFR result since the main pressure drop will be located in the stented segment, which cannot be simulated with the current algorithm that assumes complete revascularization of the stented segment. In this case, assessment of post-PCI in-stent pressure drop at the stented segment will be useful to identify the cause of suboptimal stenting results [(18)].”

Severe stent underexpansion is known to induce turbulences causing in-stent pressure losses and suboptimal post-PCI FFR results [(2)]. In the DOCTORS study, the improvement in FFR by OCT-guided PCI optimization was related mainly to the correction of stent underexpansion [(8)].

Recently, Nakamura et al. [15] reported significant correlation between stent expansion quantified by semi-automatic volumetric analysis and post-PCI FFR ($r=0.69$, $p<0.001$). Our study equally demonstrates a significant correlation between stent expansion and in-stent pressure drop, an essential observation that can be obtained from OCT pullback and OFR computation, without the need for wire-based instrumentation.

Limitations of the study

This study has several limitations. The patient profiles of the pooled studies are different: the DOCTORS study only included NSTE-ACS patients versus 31% in the OxOPT-PCI study. Although failure to achieve hyperemia in ACS patients may result in higher FFR due to microvascular dysfunction, this effect may disappear when microvascular dysfunction recovers and appears to be of marginal clinical significance in several trials, especially when interrogating non-culprit vessels [20-22]. The differences in baseline characteristics, lesion composition, study design, and medical device used could influence the study results. However, statistical analysis showed that no center bias existed between these two studies. Our results shall be interpreted with the caveat that women only represent about 10% of the included patients. Due to the retrospective design of this study, the feasibility of post-PCI OFR computation (92.8%) was not as high as in our previous prospective study (98.7%) [7], with 12 out of 167 pullbacks excluded due to insufficient image quality, mainly due to presence of image artifacts which could impair the reliability of lumen contouring. A variable degree of mismatch may exist between the distal optical sensor and distal pressure sensor

positions. This uncertainty could be a possible source of variability between post-PCI OFR and FFR. We considered the sites of distal OCT imaging and FFR measurement to be matched when there was no stenosis between the locations of both sensors. However, in practice, FFR wire is usually located at more distal position than the OCT catheter can be safely advanced. In addition, pressure loss can still be seen in some non-stenotic but atherosclerotic vessels [23]. The assumption about matching locations might have resulted in a proportion of cases with numerically lower FFR but higher OFR values. We anticipate that these "false negative" cases will be less often seen in prospective studies and perhaps reduced with the use of OCT catheters with longer pullback length. Post-PCI measurements were not confronted with follow-up data. Unlike FFR which is modulated by the downstream microcirculation and magnitude of hyperemia, OFR partially ignores the downstream microcirculatory respond. Future studies with clinical follow up data are useful to compare the clinical outcome guided by OFR versus FFR. Wire-based FFR pullbacks were not available in the present study, therefore we could only investigate the correlation between stent deployment and in-stent pressure drop from OCT and OFR pullback. Of note, Emori et al. in 103 intermediate coronary lesions demonstrated a mean pressure gradient of 0.04 within the stented segment by both FFR and OFR, with excellent agreement between post-PCI OFR and FFR in the stented segment (mean difference=0.00±0.02) [17]. Pending confirmation, it can be anticipated that our findings on the impact of stent deployment on OFR data will also be applicable to in-stent pressure drops measured by FFR.

Conclusions

Post-PCI OFR showed good correlation and excellent agreement with post-PCI wire-based FFR. Post-PCI OFR demonstrated good diagnostic concordance with post-PCI FFR. Simulated residual OFR was significantly correlated with post-PCI FFR. Stent minimum expansion index showed significant correlation with in-stent pressure drop.

Impact on daily practice

OFR immediately after PCI provides simultaneous evaluation of coronary physiology and stent expansion and apposition within a single catheter. Simulated residual OFR could be of interest to select the best stenting landmark and reference dimensions to obtain optimal functional result and to assess prior to PCI the likely degree of residual ischemia after PCI. The use of both simulated residual OFR and post-PCI OFR have the potential to inform the procedural strategy, to optimize coronary interventions and to enable complete revascularization, thereby allowing to reconcile precision PCI with the limitations imposed on reimbursement by health care systems in many geographies.

Acknowledgements

S Tu would like to acknowledge the support by the Natural Science Foundation of China [grant number 82020108015 and 81871460] and the National Key Research and Development Program of China.

Disclosures

W Wijns is supported by the Science Foundation Ireland Research Professorship grant RSF 1413. He reports research grants and honoraria from MicroPort; medical advisor of Rede Optrimus Research and co-founder of Argonauts, an innovation facilitator. AP Banning is partially funded by the NIHR Biomedical research Centre Oxford. He has an institutional grant for a fellowship from Boston scientific, speaker fees from Boston scientific, Abbott vascular and Medtronic. S Tu received research support from Pulse medical imaging technology. All other authors have reported that they have no relationships relevant to the contents of this paper to disclose.

References

1. Räber L, Mintz GS, Koskinas KC, Johnson TW, Holm NR, Onuma Y, Radu MD, Joner M, Yu B, Jia H, Meneveau N, de la Torre Hernandez JM, Escaned J, Hill J, Prati F, Colombo A, di Mario C, Regar E, Capodanno D, Wijns W, Byrne RA, Guagliumi G, Group ESD. Clinical use of intracoronary imaging. Part 1: Guidance and optimization of coronary interventions. An expert consensus document of the European Association of Percutaneous Cardiovascular Interventions. European heart journal. 2018;39:3281-3300.

2. Fearon WF, Luna J, Samady H, Powers ER, Feldman T, Dib N, Tuzcu EM, Cleman MW, Chou TM, Cohen DJ, Ragosta M, Takagi A, Jeremias A, Fitzgerald PJ, Yeung AC, Kern MJ, Yock PG. Fractional flow reserve compared with intravascular ultrasound guidance for optimizing stent deployment. Circulation. 2001;104:1917-1922.

3. Rimac G, Fearon WF, De Bruyne B, Ikeno F, Matsuo H, Piroth Z, Costerousse O, Bertrand OF. Clinical value of post-percutaneous coronary intervention fractional flow reserve value: A systematic review and meta-analysis. Am Heart J. 2017;183:1-9.

4. Leone AM, Burzotta F, Aurigemma C, De Maria GL, Zambrano A, Zimbardo G, Arioti M, Cerracchio E, Vergallo R, Trani C, Crea F. Prospective randomized comparison of fractional flow reserve versus optical coherence tomography to guide revascularization of intermediate coronary stenoses: One-month results. J Am Heart Assoc. 2019;8:e012772.

5. Yu W, Huang J, Jia D, Chen S, Raffel OC, Ding D, Tian F, Kan J, Zhang S, Yan F, Chen Y, Bezerra HG, Wijns W, Tu S. Diagnostic accuracy of intracoronary optical coherence tomography-derived fractional flow reserve for assessment of coronary stenosis severity. EuroIntervention. 2019;15:189-197.

6. Huang J, Emori H, Ding D, Kubo T, Yu W, Huang P, Zhang S, Gutiérrez-Chico JL, Akasaka T, Wijns W, Tu S. Comparison of diagnostic performance of intracoronary optical coherence tomography-based and angiography-based fractional flow reserve for evaluation of coronary stenosis. EuroIntervention. 2020;16:568-576.

7. Gutiérrez-Chico JL, Chen Y, Yu W, Ding D, Huang J, Huang P, Jing J, Chu M, Wu P, Tian F, Xu B, Tu S. Diagnostic accuracy and reproducibility of optical flow ratio for functional evaluation of coronary stenosis in a prospective series. Cardiol J. 2020;27:350-361.

8. Meneveau N, Souteyrand G, Motreff P, Caussin C, Amabile N, Ohlmann P, Morel O, Lefrancois Y, Descotes-Genon V, Silvain J, Braik N, Chopard R, Chatot M, Ecarnot F, Tauzin H, Van Belle E, Belle L, Schiele F. Optical coherence tomography to optimize results of percutaneous coronary intervention in patients with non-ST-elevation acute coronary syndrome: Results of the multicenter, randomized DOCTORS Study (Does Optical Coherence Tomography Optimize Results of Stenting). Circulation. 2016;134:906-917.

9. Wolfrum M, Maria GLD, Benenati S, Langrish J, Banning AP. What are the causes of a suboptimal FFR after coronary stent deployment? Insights from a consecutive series using OCT imaging. EuroIntervention. 2018;14:e1324-e1331.

10. Prati F, Regar E, Mintz GS, Arbustini E, Di Mario C, Jang IK, Akasaka T, Costa M, Guagliumi G, Grube E, Ozaki Y, Pinto F, Serruys PW. Expert review document on methodology, terminology, and clinical applications of optical coherence tomography: Physical principles, methodology of image acquisition, and clinical application for assessment of coronary arteries and atherosclerosis. Eur Heart J. 2010;31:401-415.

11. Prati F, Guagliumi G, Mintz GS, Costa M, Regar E, Akasaka T, Barlis P, Tearney GJ, Jang IK, Arbustini E, Bezerra HG, Ozaki Y, Bruining N, Dudek D, Radu M, Erglis A, Motreff P, Alfonso F, Toutouzas K, Gonzalo N, Tamburino C, Adriaenssens T, Pinto F, Serruys PW, Di Mario C. Expert review document part 2: Methodology, terminology and clinical applications of optical coherence tomography for the assessment of interventional procedures. Eur Heart J. 2012;33:2513-2520.

12. Prati F, Romagnoli E, Burzotta F, Limbruno U, Gatto L, La Manna A, Versaci F, Marco V, Di Vito L, Imola F, Paoletti G, Trani C, Tamburino C, Tavazzi L, Mintz GS. Clinical impact of OCT findings during PCI: The CLI-OPCI II study. J Am Coll Cardiovasc Imaging. 2015;8:1297-1305.

13. Wu P, Gutiérrez-Chico JL, Tauzin H, Yang W, Li Y, Yu W, Chu M, Guillon B, Bai J, Meneveau N, Wijns W, Tu S. Automatic stent reconstruction in optical coherence tomography based on a deep convolutional model. Biomed Opt Express. 2020;11:3374-3394.

14. Wijns W, Shite J, Jones MR, Lee SW, Price MJ, Fabbiocchi F, Barbato E, Akasaka T, Bezerra H, Holmes D. Optical coherence tomography imaging during percutaneous coronary intervention impacts physician decision-making: ILUMIEN I study. European heart journal. 2015;36:3346-3355.

15. Nakamura D, Wijns W, Price MJ, Jones MR, Barbato E, Akasaka T, Lee SW-L, Patel SM, Nishino S, Wang W, Gopinath A, Attizzani GF, Holmes D. New volumetric analysis method for stent expansion and its correlation with final fractional flow reserve and clinical outcome: An ILUMIEN I substudy. J Am Coll Cardiol Intv. 2018;11:1467-1478.

16. Toth GG, Johnson NP, Jeremias A, Pellicano M, Vranckx P, Fearon WF, Barbato E, Kern

MJ, Pijls NH, De Bruyne B. Standardization of Fractional Flow Reserve Measurements. Journal of the American College of Cardiology. 2016;68:742-753.

17. Emori H, Kubo T, Shiono Y, Ino Y, Shimamura K, Terada K, Nishi T, Higashioka D, Takahata M, Wada T, Kashiwagi M, Khalifa AKM, Tanaka A, Hozumi T, Tu S, Akasaka T. Comparison of optical flow ratio and fractional flow reserve in stent-treated arteries immediately after percutaneous coronary intervention. Circ J. 2020;84:2253-2258.

18. Ding D, Huang J, Westra J, Cohen DJ, Chen Y, Andersen BK, Holm NR, Xu B, Tu S, Wijns W. Immediate post-procedural functional assessment of percutaneous coronary intervention: current evidence and future directions. European heart journal. 2021;0:1-16.

19. Tu S, Westra J, Yang J, von Birgelen C, Ferrara A, Pellicano M, Nef H, Tebaldi M, Murasato Y, Lansky A, Barbato E, van der Heijden LC, Reiber JHC, Holm NR, Wijns W. Diagnostic accuracy of fast computational approaches to derive fractional flow reserve from diagnostic coronary angiography: The international multicenter FAVOR Pilot study. J Am Coll Cardiol Intv. 2016;9:2024-2035.

20. Tu S, Westra J, Adjedj J, Ding D, Liang F, Xu B, Holm NR, Reiber JHC, Wijns W. Fractional flow reserve in clinical practice: from wire-based invasive measurement to image-based computation. European heart journal. 2020;41:3271-3279.

21. Engstrøm T, Kelbæk H, Helqvist S, Høfsten DE, Kløvgaard L, Holmvang L, Jørgensen E, Pedersen F, Saunamäki K, Clemmensen P, De Backer O, Ravkilde J, Tilsted HH, Villadsen AB, Aarøe J, Jensen SE, Raungaard B, Køber L. Complete revascularisation versus treatment of the culprit lesion only in patients with ST-segment elevation myocardial infarction and multivessel disease (DANAMI-3—PRIMULTI): An open-label, randomised controlled trial.

Lancet. 2015;386:665-671.

22. Smits PC, Abdel-Wahab M, Neumann FJ, Boxma-de Klerk BM, Lunde K, Schotborgh CE, Piroth Z, Horak D, Wlodarczak A, Ong PJ, Hambrecht R, Angerås O, Richardt G, Omerovic E. Fractional Flow Reserve-Guided Multivessel Angioplasty in Myocardial Infarction. The New England journal of medicine. 2017;376:1234-1244.

23. De Bruyne B, Hersbach F, Pijls NHJ, Bartunek J, Bech JW, Heyndrickx GR, Gould KL, Wijns W. Abnormal Epicardial Coronary Resistance in Patients With Diffuse Atherosclerosis but "Normal" Coronary Angiography. Circulation. 2001;104:2401-2406.

Figure Legends

Central Illustration. Computation of simulated residual OFR, post-PCI OFR, and quantification of stent expansion and apposition.

Top: Computation of simulated residual OFR using pre-PCI OFR pullback. (A1) Coronary angiography of LAD before PCI. FFR measured at asterisk was 0.64. (A2) 3D reconstructed artery. The OCT images at the proximal reference lumen, stenotic lesion(s), and distal reference lumen were shown in I, II, III, and IV, respectively. (A3) The computed OFR along the vessel is presented by a virtual pressure pullback for co-registration between pressure-drop and anatomy. OFR of the interrogated vessel was 0.63, with drop of OFR in the selected lesion (Lesion OFR) of 0.30. Simulated residual OFR was calculated as 0.93. **Middle and Bottom**: Computation of post-PCI OFR and quantification of stent expansion and apposition. (B1) Coronary angiography of LAD after PCI. FFR measured at asterisk was 0.84. (B2) 3D reconstructed artery and the implanted stent. (B3) Computed OFR pullback co-registered with anatomy. Vessel OFR was 0.85, with drop of OFR inside the stent (In-stent OFR) of 0.08. (B4) Distribution of stent expansion index and maximum malapposition distance of each frame along the stented segment. Frame 245 had MEI (shown in III) while frame 247 had maximum strut-lumen distance (shown in II).

FFR = fractional flow reserve; LAD = left anterior descending artery; MEI = minimum expansion index; OCT = optical coherence tomography; OFR = optical flow ratio; PCI = percutaneous coronary intervention.

Figure 1. Study flow chart.

FFR = fractional flow reserve; OCT = optical coherence tomography; OFR = optical flow ratio; PCI = percutaneous coronary intervention.

Figure 2. Correlation and agreement between post-PCI OFR and FFR.

Abbreviations as in Figure 1.

Figure 3. ROC Curves for predicting post-PCI FFR≤0.90.

AUC = area under the ROC curve; ROC = receiver-operating characteristics; MLA = minimal lumen area; other abbreviations as in Figure 1.

Figure 4. Correlation and agreement between simulated residual OFR and post-PCI FFR.

Abbreviations as in Figure 1.

Tables

Table 1. Baseline demographic and vessel characteristics

	Paired post-PCI OFR and FFR
Per patient	**N = 119**
Age, years	64.6 ± 10.3
Women	15 (12.6%)
BMI, kg/m^2 *	28.1 ± 4.9
Diabetes mellitus	25 (21.0%)
Hypertension	71 (59.7%)
Hypercholesterolemia	62 (52.1%)
Current smoker	40 (33.6%)
Previous smoker	31 (26.1%)
Family history of CAD	33 (27.7%)
Previous PCI	19 (16.0%)
Previous CABG	1 (0.8%)
Previous MI	21 (17.6%)
Clinical presentation	
Stable angina	12 (10.1%)
Unstable angina	11 (9.2%)
NSTEMI	89 (74.8%)

Staged PCI	7 (5.9%)
Per vessel	**N = 119**
Lesion location	
LAD	61 (51.3%)
LCx	25 (21.0%)
RCA	33 (27.7%)
Per pullback	**N = 125**
QCA parameters	
DS%	26.6 ± 6.8
MLD	2.07 ± 0.50
Lesion length, mm	13.9 ± 8.2
Reference vessel diameter, mm	2.81 ± 0.61
Diffuse lesion	7 (5.6%)
Tandem lesion	0 (0.0%)
Calcified lesion	81 (64.8%)
Bifurcation lesion	28 (22.4%)
Post-PCI FFR	
Mean ± SD	0.92 ± 0.05
Median [quartiles]	0.93 [0.89, 0.96]
FFR ≤0.90	36 (28.8%)
FFR ≤0.80	4 (3.2%)

Post-PCI OFR	
Mean ± SD	0.93 ± 0.05
Median [quartiles]	0.94 [0.91, 0.97]
OFR ≤0.90	28 (22.4%)
OFR ≤0.80	4 (3.2%)
MLA, mm^2	3.68 [2.94, 5.36]
MSA, mm^2	5.56 [4.47, 7.08]
Stent length, mm	25.5 ± 11.7

Data are presented as mean ± standard deviation, median [quartiles] or number (percentage). *: 115 patients. BMI = body mass index; CABG = coronary artery bypass grafting; CAD = coronary artery disease; DS% = percent diameter stenosis; FFR = fractional flow reserve; LAD = left anterior descending artery; LCx = left circumflex; MI = myocardial infarction; MLA = minimal lumen area; MLD = minimum lumen diameter; MSA = minimum stent area; NSTEMI = non-ST-segment elevation myocardial infarction; OFR = optical flow ratio; PCI = percutaneous coronary intervention; QCA = quantitative coronary angiography; RCA = right coronary artery; SD = standard deviation.

Table 2. Performance of post-PCI OFR and OCT-derived MLA in predicting FFR ≤0.90

	Post-PCI OFR ≤0.90	**MLA ≤3.28 mm^2**
Accuracy, % (95% CI)	84 (77, 91)	71 (63, 79)
Sensitivity, % (95% CI)	61 (44, 77)	64 (46, 79)
Specificity, % (95% CI)	93 (86, 98)	74 (64, 83)
PPV, % (95% CI)	79 (59, 92)	50 (35, 65)
NPV, % (95% CI)	86 (77, 92)	84 (74, 91)
+LR (95% CI)	9.1 (4.0, 20.5)	2.5 (1.6, 3.8)
-LR (95% CI)	0.42 (0.30, 0.60)	0.49 (0.30, 0.80)

Data for +LR and -LR are presented as ratio (95% CI) and for the rest of parameters as % (95% CI). CI = confidence interval; MLA = minimal lumen area; NPV = negative predictive value; PPV = positive predictive value; OCT = optical coherence tomography; +LR = positive likelihood ratio; –LR = negative likelihood ratio; other abbreviations as in Table 1.

Central Illustration

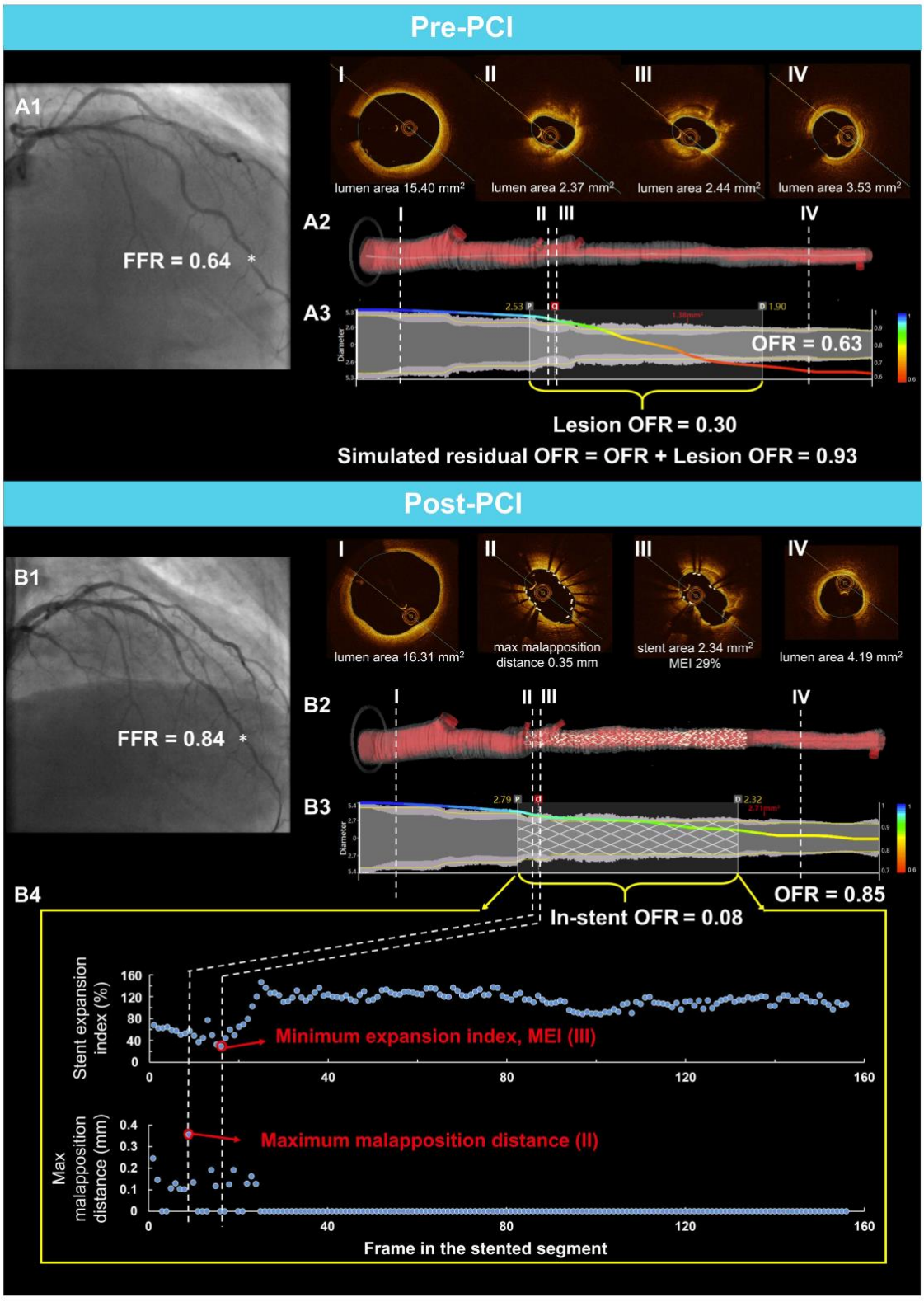

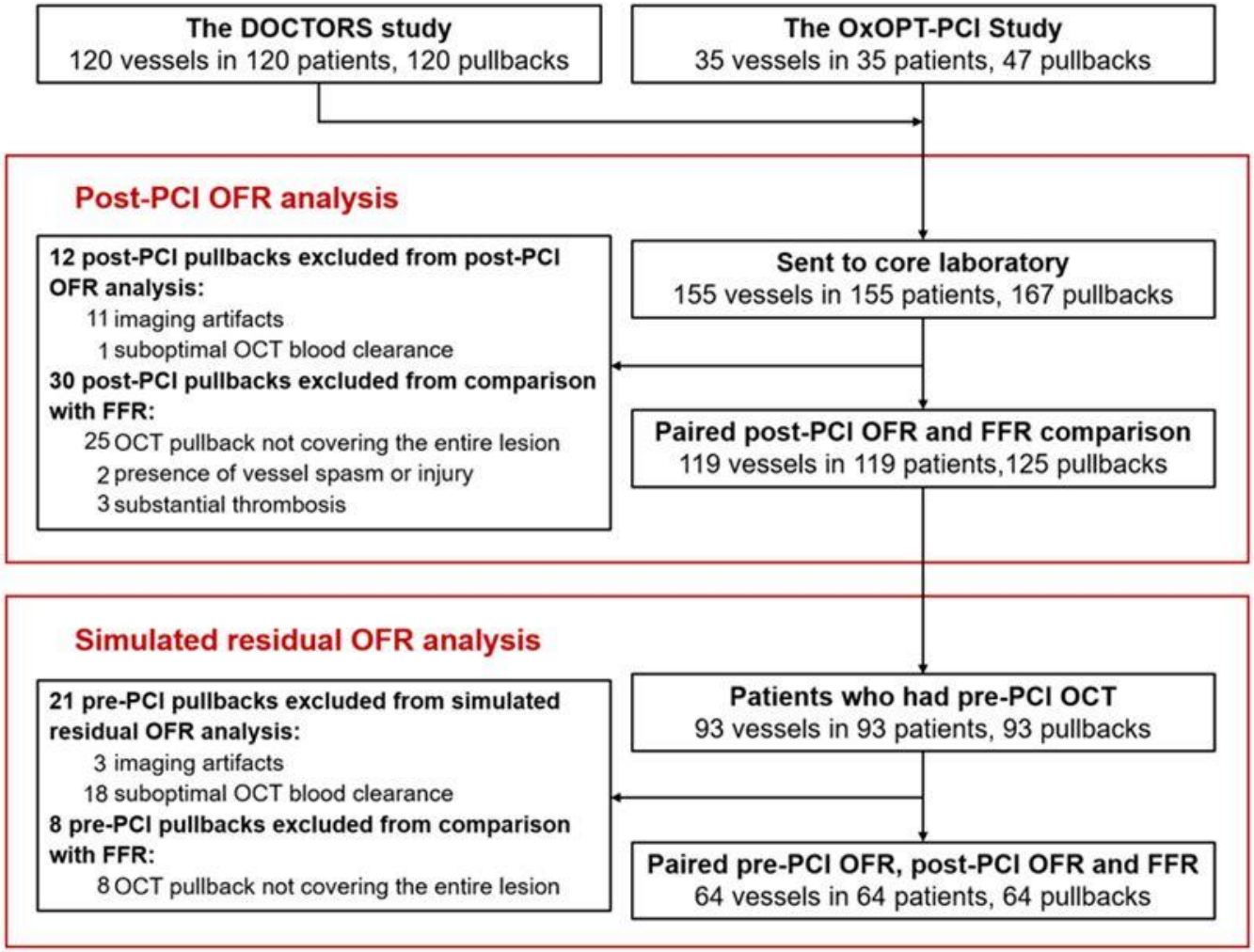

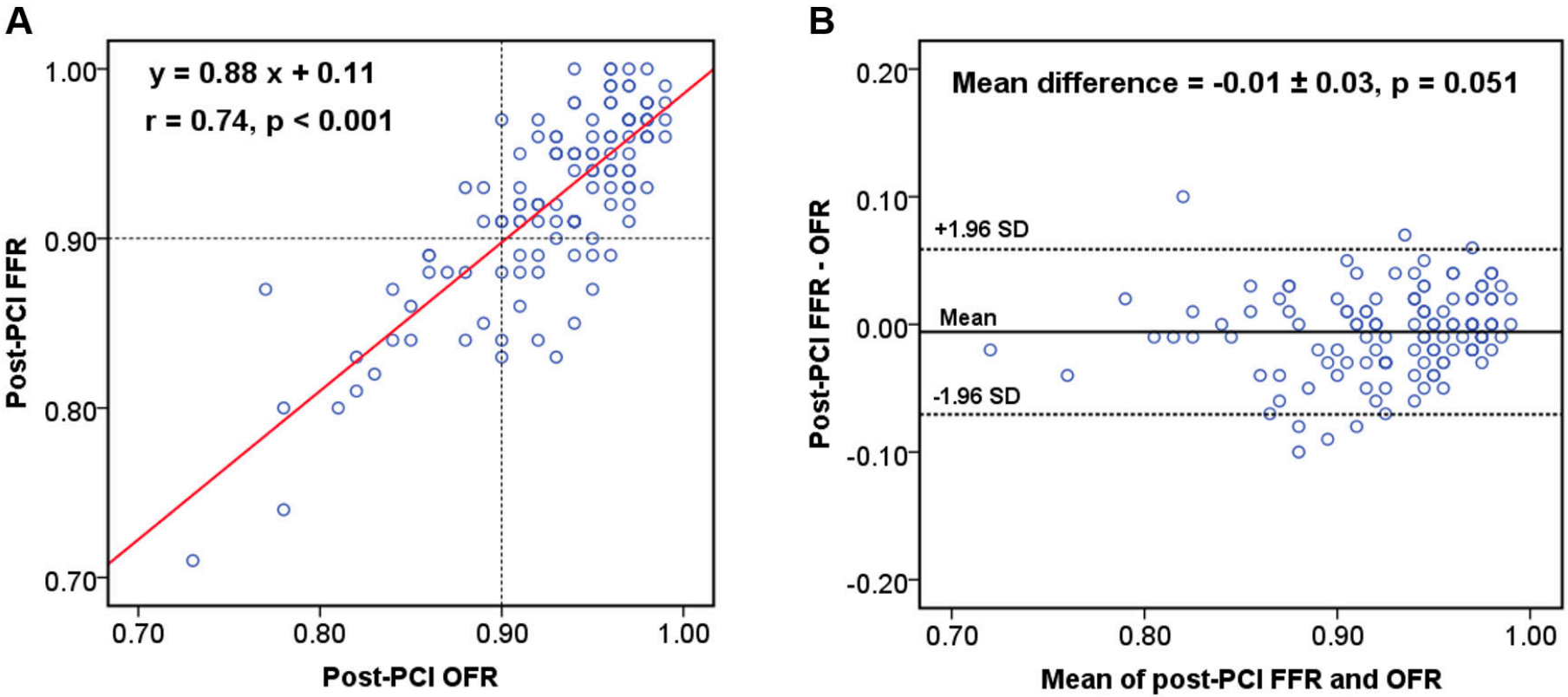

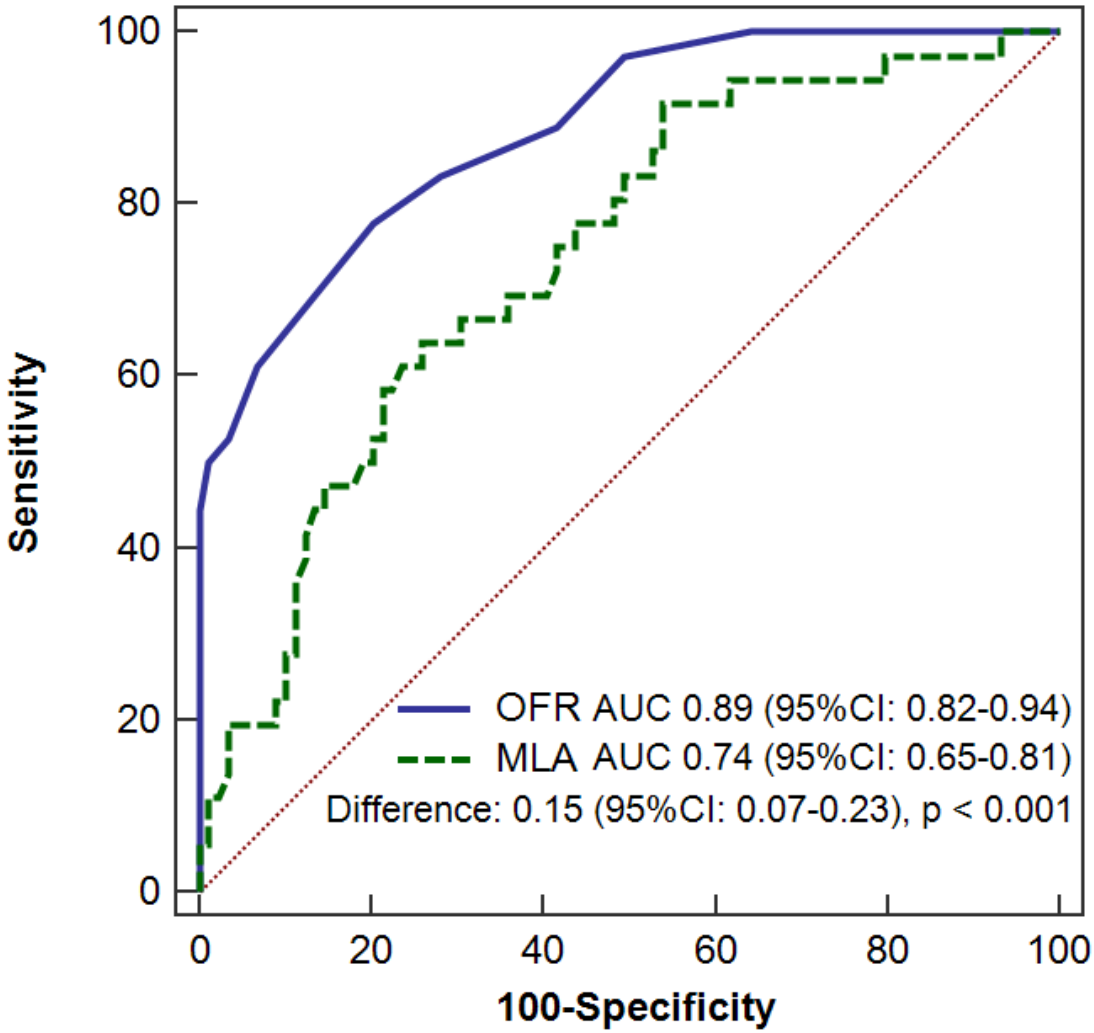

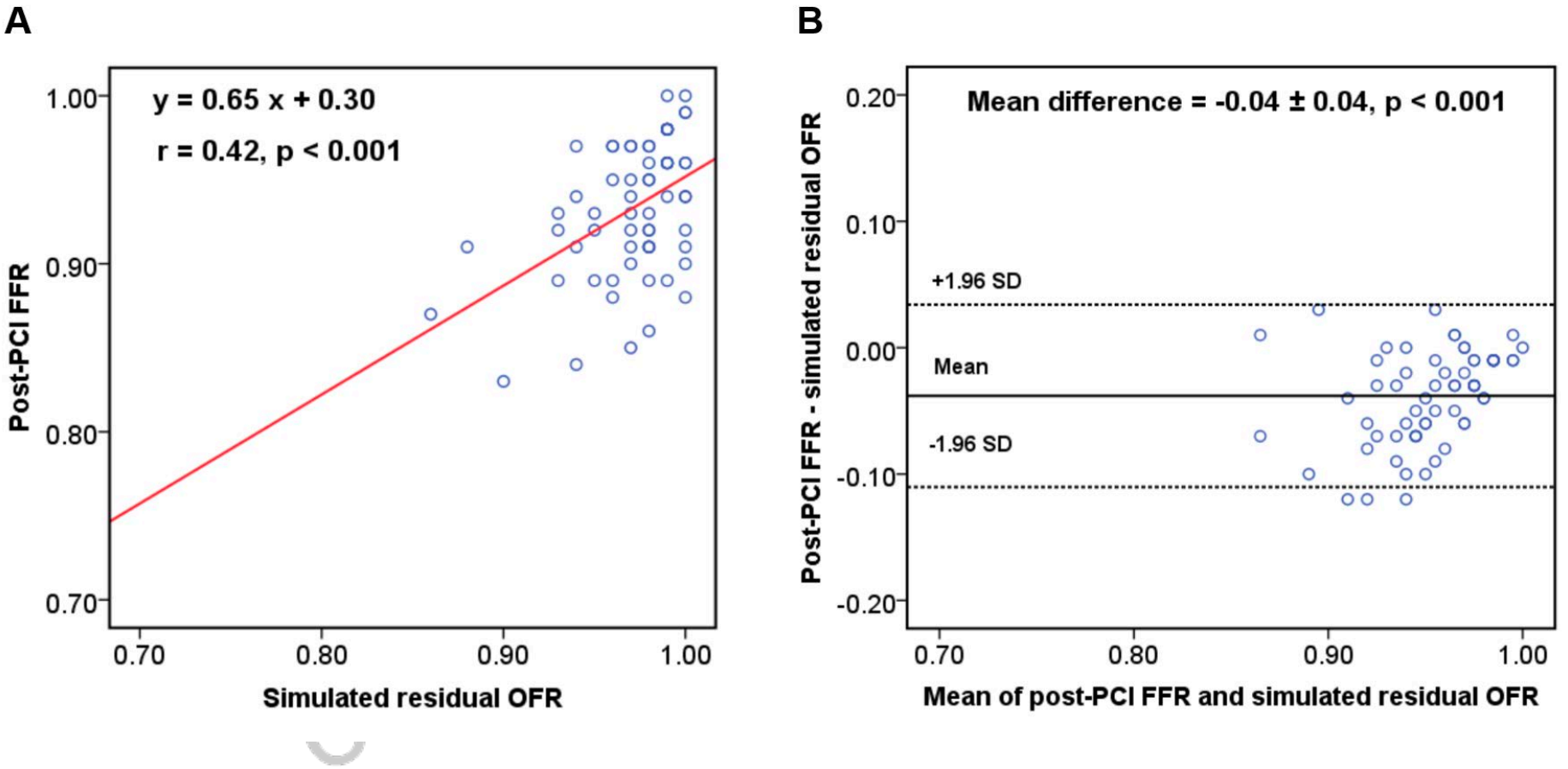

SUPPLEMENTARY MATERIAL

OCT image acquisition and analysis

Details for OCT measurement were reported in the main studies [8,9]. Optical coherence tomography imaging was performed using frequency-domain (FD) OCT systems (ILUMIEN™ OPTIS™; St. Jude Medical/Abbott, Saint Paul, MN, USA) with Dragonfly™ Duo Imaging Catheter, or FD-OCT Optis system (Lightlab Imaging Incorporated, Westford, MA) with Dragonfly Duo and Dragonfly Optis catheter. OCT imaging was performed on a 54 mm length segment. The OCT catheter was pulled back automatically at a speed of 18 mm/second using a non-occlusive technique. Cross-sectional images were generated at a rotational speed of 100 frames/second or 180 frames/second.

OCT-detected quantitative and qualitative features including stent malapposition, stent underexpansion, tissue protrusions, thrombi, and stent edge dissections were performed according to the definitions in recent recommendations [10,11] (**Supplementary Material**). OCT images were analyzed using OctPlus software (version 2.0, Pulse Medical Imaging Technology, Shanghai, China) in the core laboratory.

Definitions of OCT criteria for qualitative and quantitative features

OCT-detected features including stent malapposition, tissue protrusions, thrombi, and stent edge dissections were performed according to the definitions in recent recommendations [10,11].

- **Stent malapposition** was defined as >200 μm in stent-adjacent vessel lumen distance.
- **Stent underexpansion** was defined as a minimal stent area <70% of the average reference area.
- **Intra-stent tissue prolapse** was defined as the intraluminal protrusion of tissue between implanted stent struts with thickness ≥500 μm.
- **Incomplete lesion coverage** was defined as plaque 10 mm proximal or distal to stent edges with reference lumen area <4.5 mm^2.
- **Thrombus** was identified as an intra-luminal mass, with no direct continuity with the surface of the vessel wall or as a highly backscattered luminal protrusion in continuity with the vessel wall and resulting in signal-free shadowing [12].
- **Stent edge dissection** was identified if dissection flap was ≥200 μm.

Supplementary Table 1. Baseline demographic and vessel characteristics

	Paired simulated residual OFR, post-PCI OFR and FFR
Per patient	**N = 64**
Age, years	64.2 ± 10.8
Women	7 (10.9%)
BMI, kg/m^2	27.1 ± 4.6
Diabetes mellitus	10 (15.6%)
Hypertension	30 (46.9%)
Hypercholesterolemia	30 (46.9%)
Current smoker	27 (42.2%)
Previous smoker	14 (21.9%)
Family history of CAD	18 (28.1%)
Previous PCI	6 (9.4%)
Previous CABG	0 (0.0%)
Previous MI	7 (10.9%)
Clinical presentation	
Stable angina	1 (1.6%)
Unstable angina	5 (7.8%)
NSTEMI	56 (87.5%)
Staged PCI	2 (3.1%)

Per vessel	**N = 64**
Lesion location	
LAD	36 (56.3%)
LCx	9 (14.1%)
RCA	19 (29.7%)
Per pullback	**N = 64**
QCA parameters	
DS%	24.5 ± 6.6
MLD	2.09 ± 0.46
Lesion length, mm	12.6 ± 7.7
Reference vessel diameter, mm	2.76 ± 0.57
Diffuse lesion	2 (3.1%)
Tandem lesion	0 (0.0%)
Calcified lesion	43 (67.2%)
Bifurcation lesion	16 (25.0%)
Post-PCI FFR	
Mean ± SD	0.93 ± 0.04
Median [quartiles]	0.94 [0.91, 0.97]
FFR ≤0.90	14 (21.9%)
FFR ≤0.80	0 (0.0%)
Post-PCI OFR	

Mean ± SD	0.94 ± 0.04
Median [quartiles]	0.94 [0.92, 0.97]
OFR ≤0.90	8 (12.5%)
OFR ≤0.80	0 (0.0%)
Simulated residual OFR	
Mean ± SD	0.97 ± 0.03
Median [quartiles]	0.98 [0.96, 0.99]
MLA, mm^2	4.38 [3.18, 5.86]
MSA, mm^2	5.88 [4.56, 7.47]
Stent length, mm	24.1 ± 11.7

Data are presented as mean ± standard deviation, median [quartiles] or number (percentage). BMI = body mass index; CABG = coronary artery bypass grafting; CAD = coronary artery disease; DS% = percent diameter stenosis; FFR = fractional flow reserve; LAD = left anterior descending artery; LCx = left circumflex; MI = myocardial infarction; MLA = minimal lumen area; MLD = minimum lumen diameter; MSA = minimum stent area; NSTEMI = non-ST-segment elevation myocardial infarction; OFR = optical flow ratio; PCI = percutaneous coronary intervention; QCA = quantitative coronary angiography; RCA = right coronary artery; SD = standard deviation.

Supplementary Table 2. Qualitative and quantitative features by OCT and impact on diagnostic concordance between OFR and FFR*

		Variable present	Variable absent	P value
Thrombus (%)	n (%)	65 (52.0%)	60 (48.0%)	
	accuracy	81.5 (71.9, 91.2)	86.7 (77.8, 95.5)	0.591
Stent malapposition (%)	n (%)	44 (35.2%)	81 (64.8%)	
	accuracy	90.0 (82.1, 99.8)	80.3 (71.4, 89.1)	0.194
Stent underexpansion (%)	n (%)	38 (30.4%)	87 (69.6%)	
	accuracy	89.5 (79.3, 99.7)	81.6 (73.3, 89.9)	0.402
Tissue protrusion (%)	n (%)	48 (38.4%)	77 (61.6%)	
	accuracy	85.4 (75.1, 95.8)	83.2 (74.6, 91.7)	0.928
Stent edge dissection (%)	n (%)	36 (28.8%)	89 (71.2%)	
	accuracy	86.1 (74.2, 98.0)	83.2 (75.2, 91.1)	0.889
Incomplete lesion coverage (%)	n (%)	7 (5.6%)	118 (94.4%)	
	accuracy	85.7 (50.8, 100.0)	84.0 (77.2, 90.6)	0.687

*Diagnostic concordance is calculated for post-PCI FFR ≤0.90 and post-PCI OFR ≤0.90.

Supplementary Table 3. Performance of simulated residual OFR in predicting post-PCI FFR ≤0.90

	Simulated residual OFR ≤0.90
Accuracy, % (95% CI)	80 (70, 90)
Sensitivity, % (95% CI)	14 (2, 43)
Specificity, % (95% CI)	98 (89, 100)
PPV, % (95% CI)	67 (9, 99)
NPV, % (95% CI)	80 (68, 89)
+LR (95% CI)	7.1 (0.7, 73.1)
-LR (95% CI)	0.87 (0.70, 1.10)

Data for +LR and -LR are presented as ratio (95% CI) and for the rest of parameters as % (95% CI). CI = confidence interval; FFR = fractional flow reserve; NPV = negative predictive value; OFR = optical flow ratio; PCI = percutaneous coronary intervention; PPV = positive predictive value; +LR = positive likelihood ratio; -LR = negative likelihood ratio.

Supplementary Figure 1. An example case comparing evaluation of stent expansion by Nakamura et al. [15] and by our method.

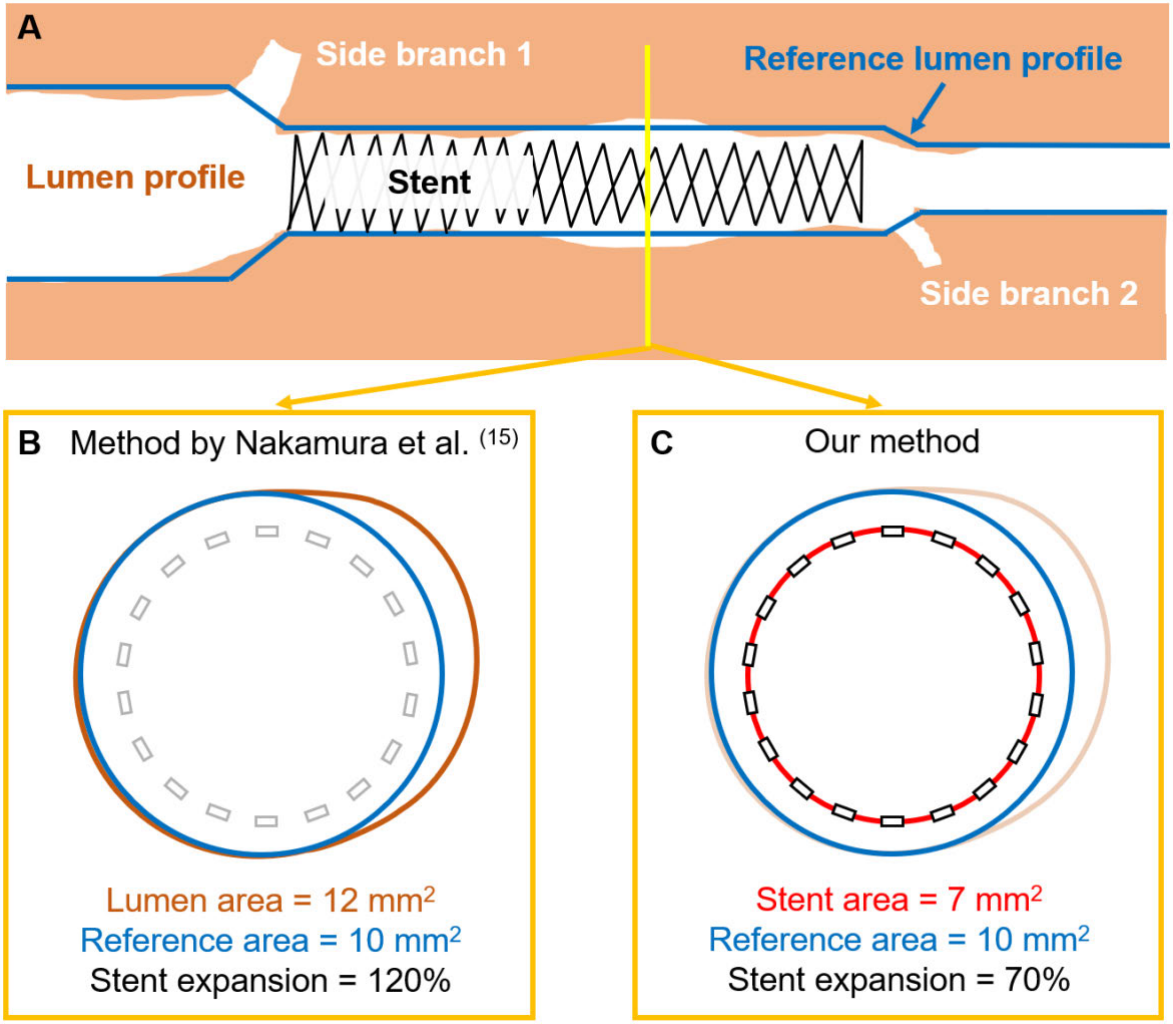

(A) Lumen profile of an interrogated vessel with two major side branches after PCI. Reference lumen profile (delineated in blue lines) was developed considering the step-down phenomenon across bifurcations. Notably the lumen at the middle of the stented segment was larger than corresponding reference lumen due to positive vessel remodeling. The cross-section of the frame indicated by the yellow line was shown in (B) and (C). Using the method by Nakamura et al. [15], stent expansion was calculated as lumen area divided by

reference area, being 120%, indicating stent over-expansion. However, using our method, stent expansion was calculated as stent area divided by reference area, being 70%, indicating stent underexpansion.

Supplementary Figure 2. Distribution of paired post-PCI OFR and FFR (125 pullbacks).

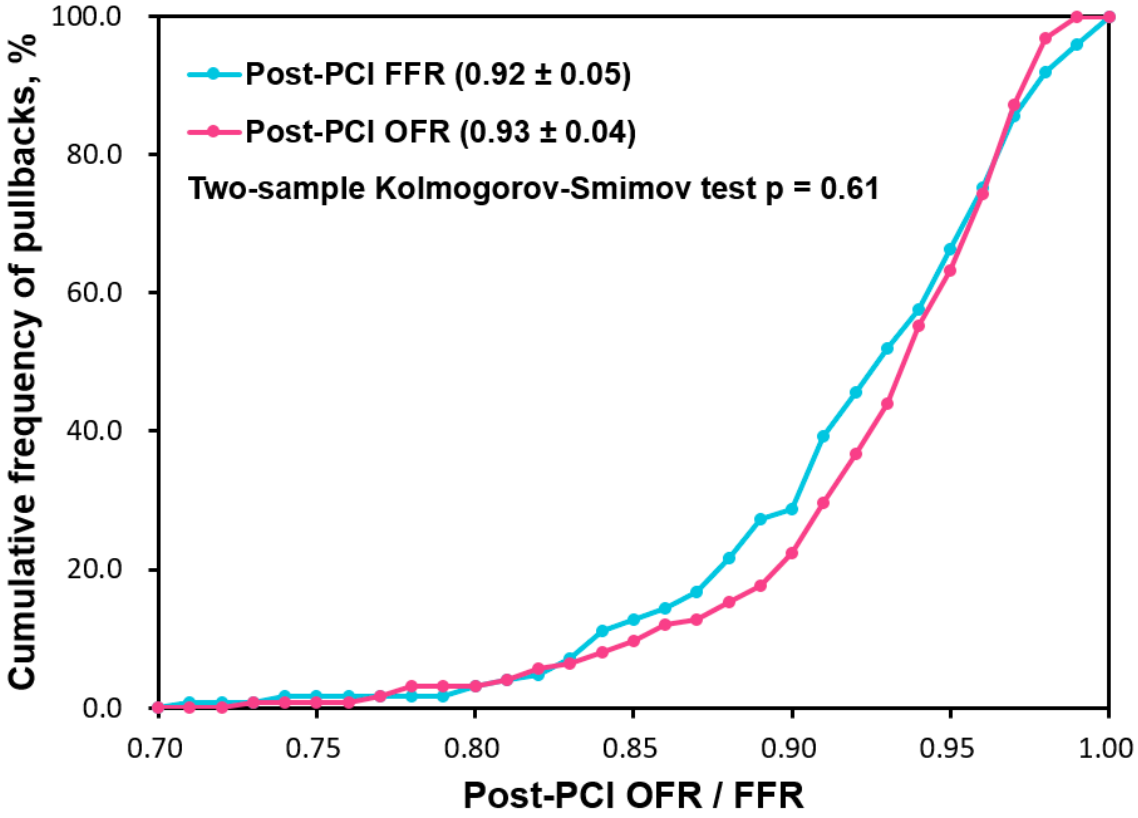

FFR = fractional flow reserve; OFR = optical flow ratio.

Supplementary Figure 3. Impact of OCT-detected qualitative and quantitative features on paired difference between post-PCI OFR and FFR.

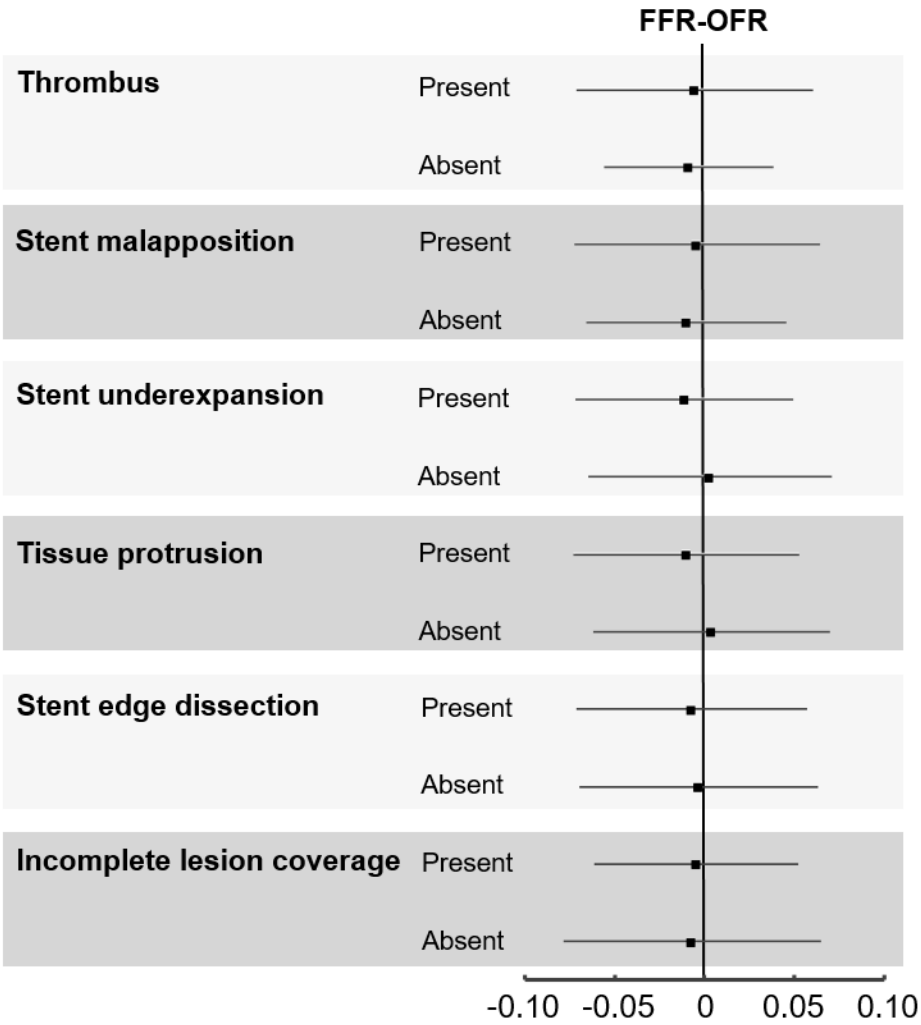

Paired difference between FFR and OFR was independent from the presence of OCT-detected stent malapposition, stent underexpansion, tissue protrusion, thrombi, stent edge dissection, and incomplete lesion coverage. Abbreviations as in Supplementary Figure 2.

Supplementary Figure 4. Correlation of stent minimum expansion index (MEI) and stent malapposition with in-stent pressure drop (In-stent OFR).

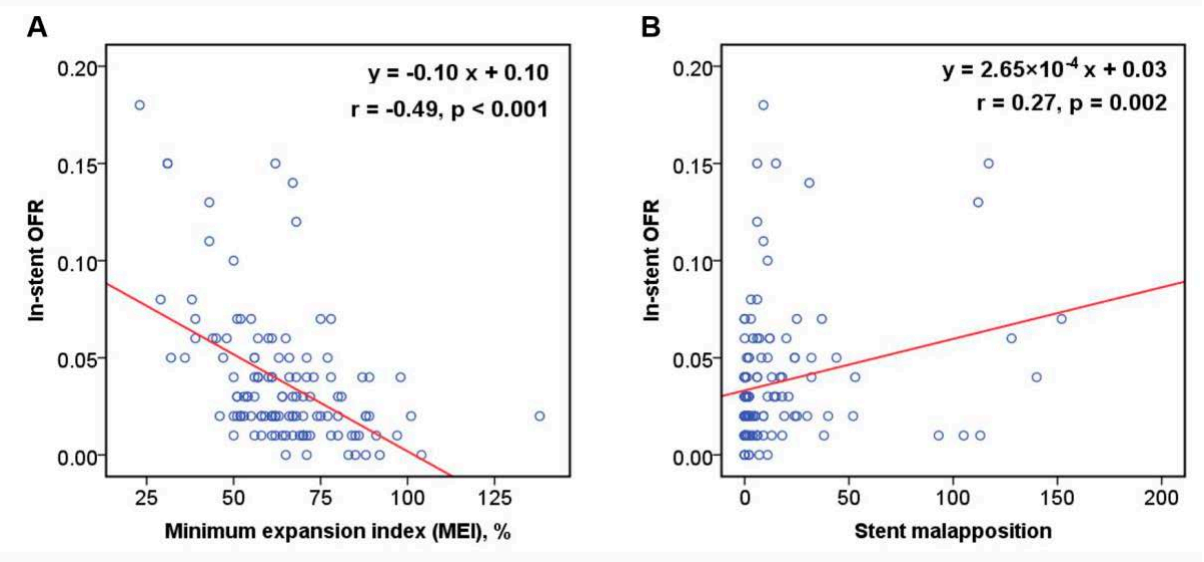

Both stent minimum expansion index (MEI) and stent malapposition significantly correlated with in-stent pressure drop. Abbreviations as in Supplementary Figure 2.